MODEL-BASED DESIGN OF STIMULUS TRAINS FOR SELECTIVE MICROSTIMULATION OF TARGETED NEURONAL POPULATIONS

Cameron C. McIntyre and Warren M. Grill

Department of Biomedical Engineering
Case Western Reserve University, OH, USA

Abstract-**Selective activation of targeted neuronal populations is required for central nervous system (CNS) neuroprosthetic device efficacy. However in many regions of the CNS, cells and fibers of passages are intermingled. The goal of this project was to design stimulus trains that would enhance selectivity between microstimulation of cells and fibers of passage. Detailed computer-based models were developed that accurately reproduced the dynamic firing properties of mammalian neurons. The neuron models were coupled to a three-dimensional finite element model of the spinal cord that solved for the potentials generated in the tissue medium by an extracellular electrode. The results demonstrate that alterations in the stimulus frequency, based on differences in the post-action-potential recovery cycles of cells and axons, enabled differential activation of cells or fibers of passage. The results also show that asymmetrical charge-balanced biphasic stimulus waveforms, designed to exploit the non-linear conductance properties of the neural elements, can be used in combination with the appropriate stimulus frequency to further enhance selectivity. These outcomes provide useful tools for selective stimulation of the CNS, as well as basis for understanding frequency-dependent outputs during CNS stimulation.**
Keywords - **neuron model, finite element model, electrode**

I. INTRODUCTION

Microstimulation in the central nervous system (CNS) can activate populations of neurons with greater specificity than is possible with larger electrodes on the surface of the spinal cord or brain [1,2]. The potential thus arises for electrical activation of intact neuronal circuitry, and in turn, generation of distributed and controlled motor outputs for application in neural prostheses [3]. Selective activation of targeted populations is required for device efficacy. However in many regions of the CNS, cells and fibers of passages are intermingled and the thresholds of cells and fibers in close proximity to the electrode are similar with conventional stimuli [1,4].

We have previously developed asymmetrical charge-balanced biphasic stimuli that increased the selectivity between local cells and fibers of passage [5]. However this analysis was limited to idealized neural orientations and single stimuli. Neural prostheses use trains of stimuli with frequencies that range from 10-150 Hz. Therefore, we developed computer-based models of cells and fibers that could reproduce the dynamic firing properties of mammalian CNS neurons. These neuron models were coupled to a three-dimensional finite element model of the spinal cord that solved for the potentials generated in the tissue medium by an extracellular electrode.

The goals of this study were to answer three questions related to the development of effective stimulus trains for CNS neuroprosthetic devices. 1) Are the selective stimulation waveforms developed in our previous work [5] effective in a specific neuroprosthetic application? 2) Are these waveforms effective when used in a high frequency stimulus train? and 3) What is the influence of synaptic inputs on excitation of cells near the electrode?

The results demonstrate that the appropriate choice of stimulus waveform and frequency, based on geometrical and electrical differences in the different target neuronal elements as well as changes in excitability that occur following their respective action potentials, provide effective techniques to improve selectivity between neural populations. The results also indicate that when stimulating local cells near the electrode that thresholds for pre-synaptic inputs are less than thresholds for direct activation of the post-synaptic cell and, as a result, post-synaptic potentials can play a role in the excitability of local cells at high stimulus frequencies.
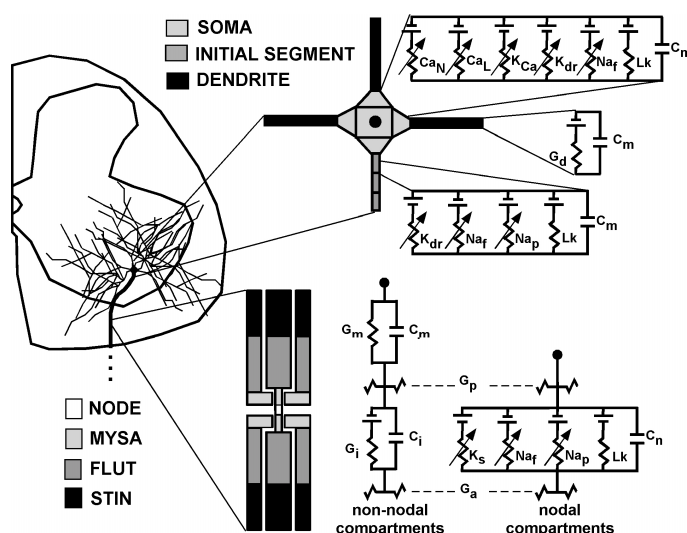
Fig. 1. Motoneuron model. Multi-compartment cable model consisted of a branching dendritic tree, multi-compartment soma and initial segment, and a myelinated axon with explicit representation of the myelin and underlying axolemma. The soma, initial segment and nodes of Ranvier used non-linear membrane dynamics derived from experimental measurements of mammalian neurons. Intracellular resisters determined by the dimensions of the adjoining compartments connected the different elements of the model together.

II. METHODS

This project used an integrated field-neuron model to study neural activation by stimulation with microelectrodes within the spinal cord. Three-dimensional (3-D) multi-compartment cable models of spinal motoneurons were generated with branching dendritic trees, multicompartment cell bodies and myelinated

Report Documentation Page

Report Date	Report Type	Dates Covered (from... to)
25 Oct 2001	N/A	-

Title and Subtitle	Contract Number
Model-Based Design of Stimulus Trains for Selective Microstimulation of Targeted Neuronal Populations	Grant Number
	Program Element Number

Author(s)	Project Number
	Task Number
	Work Unit Number

Performing Organization Name(s) and Address(es)	Performing Organization Report Number
Department of Biomedical Engineering Case Western Reserve University, OH	

Sponsoring/Monitoring Agency Name(s) and Address(es)	Sponsor/Monitor's Acronym(s)
US Army Research, Development & Standardization Group (UK) PSC 802 Box 15 FPO AE 09499-1500	Sponsor/Monitor's Report Number(s)

Distribution/Availability Statement
Approved for public release, distribution unlimited

Supplementary Notes
Papers from 23rd Annual International Conference of the IEEE Engineering in Medicine and Biology Society, October 25-28, 2001, held in Istanbul Turkey. See also ADM001351 for entire Conference on cd-rom.

Abstract

Subject Terms

Report Classification	Classification of this page
unclassified	unclassified

Classification of Abstract	Limitation of Abstract
unclassified	UU

Number of Pages
4

axons including explicit representation of the myelin sheath (Fig. 1). The geometry and membrane properties of the neural models were based upon experimental results from mammalian motoneurons. A 3-D finite element model of the spinal cord was used to calculate the potential distribution generated in the spinal cord by intraspinal microelectrodes (Fig. 2). These potentials were then applied to the neuron models to predict excitation using equivalent intracellularly injected currents [5,6].
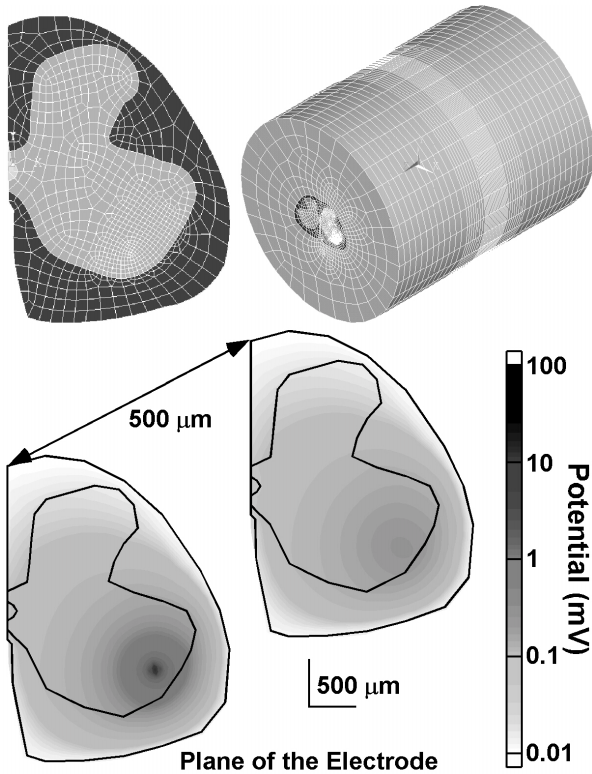
Fig. 2. Spinal cord model. A finite element model, incorporating the inhomogenous and anisotropic tissue properties of the spinal cord, was generated and used to solve for the potential distribution generated by microstimulation in the ventral horn. A non-uniform mesh, both cross-sectionally and longitudinally, was used to allow for improved accuracy near the electrode where the gradient of the electric field was the greatest. Potential distribution plotted for a 1 μA stimulus.

We modeled microstimulation near Onuf's nucleus in the ventral horn of the S2-S3 region of the cat spinal cord. The axons of the preganglionic parasympathetic innervation of the bladder run in close proximity to the cell bodies of the somatic motoneurons innervating the external urethral sphincter [7,8]. Neuron models were integrated into the volume conductor model of the spinal cord with anatomical locations based on experimental tracing studies allowing for comparisons of three different situations (Fig. 3): Activation of neurons with their cell bodies near the electrode (representative of neurons controlling the external urethral sphincter), activation of

neurons with their axons passing by the electrode but with their cell bodies within ~1000 μm of the electrode (representative of neurons controlling the bladder), and activation of fibers of passage whose cell bodies were far from the electrode (representative of fibers of passage in the white matter). The three neuron models were positioned such that the thresholds for excitation from a single symmetrical, charge-balanced, cathode first, anode second, biphasic stimulus 0.2 ms in duration was 34 μA. This enabled comparison of changes in the neuronal output with alteration in the stimulus frequency and stimulus waveform from a reference point that represents the most commonly used stimulus waveform in neuroprosthetic applications.

III. RESULTS

The neuron models were able to replicate a wide range of experimental data from mammalian motoneurons including input resistance, time constant, and action potential shape. Most importantly for dynamic firing properties, the models accurately reproduced the shape of the depolarizing and hyperpolarizing afterpotentials measured experimentally in both the cell body and myelinated axon. As a result, the models were able to match experimental records on post-action potential excitability, as well as spike frequency adaptation and steady-state repetitive discharge in response to a constant current stimulus.

The neuron models were used to predict excitation using trains of stimuli applied to the spinal cord model. We hypothesized that due to differences between the post-action potential recovery cycles of cells and axons, that selectivity could be enhanced by an appropriate choice of stimulus frequency. Neuronal output was quantified as the percentage of stimuli in the train that generated propagating action potentials in the neurons. Figure 3A shows the neuronal output of each of the three different neurons for symmetrical biphasic stimulus trains of 25-150 Hz and 25-50 μA amplitudes. The results demonstrate that modulation of the frequency of the stimulus train enhanced selectivity between activation of cells and fibers of passage within the CNS.

Selectivity of either the local cell or fibers of passage could be improved using asymmetrical charge-balanced biphasic stimuli. When an asymmetrical charge-balanced biphasic cathode first anode second stimulus waveform designed to selectively activate the cells near the electrode [5] was used there was a decrease in the threshold for activation of the cell near the electrode and there was no activation of either of the fibers of passage for the stimulus amplitude range tested (Fig. 3B). When an asymmetrical charge-balanced biphasic anode first cathode second stimulus waveform designed to selectively activate fibers of passage near the electrode [5] was used there was enhanced activation of the fibers of passage with no activation of the local cell (Fig. 3C).
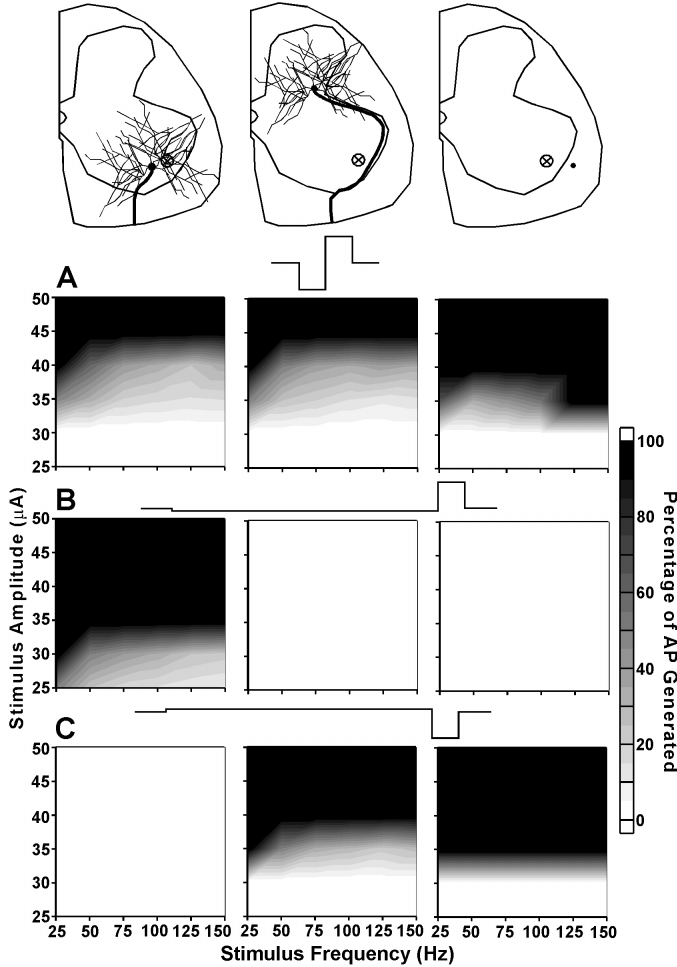
Fig. 3. Neuronal output as a function of stimulus amplitude and frequency. Neuronal output (percentage of stimuli in the stimulus train that generate propagating action potentials (AP) in the neuron models) was quantified for three different neurons for three different stimulus waveforms. A) Neuronal output for a charge-balanced symmetrical biphasic (100 μs pulse duration for each phase, no interphase delay) cathode first anode second stimulus train. B) Neuronal output for a charge-balanced asymmetrical biphasic (no interphase delay) cathode first (1000 μs pulse duration) anode second (100 μs pulse duration) stimulus train designed to selectively activated local cells. C) Neuronal output for a charge-balanced asymmetrical biphasic (no interphase delay) anode first (1000 μs pulse duration) cathode second (100 μs pulse duration) stimulus train designed to selectively activated fibers of passage.

Previous experimental results suggest that the threshold for indirect, or transsynaptically evoked action potentials, is similar to the threshold for direct excitation of the neuron with extracellular sources [2]. We developed a model of synaptic input on our motoneuron model to determine the potential roles of indirect activation of local cells by extracellular stimulus trains (Fig. 4). Action potentials were evoked at all eight boutons of the pre-synaptic input and the pre-synaptic fibers followed the stimulus frequency 100% for the extracellular stimuli examined. After the onset of extracellular stimulus pulse there was a 2 ms delay before onset of the synaptic potential in the motoneuron, representative of activation of the pre-synaptic fiber, transmitter release, and post-synaptic channel activation.

The output map of the motoneuron with excitatory synaptic input (Fig. 4A) was only slightly different than the map without the synaptic input (Fig. 3). The excitatory post-synaptic potential (PSP) reached peak amplitude of 4.5 mV, 1.5 ms after onset and lasted 10 ms, as recorded in the soma [9]. Therefore, for the stimulus frequencies examined in this study, the synaptic influence from the previous pulse was minimal by the onset of the next pulse. However, inhibitory synaptic action has a longer time course. An inhibitory PSP was implemented that reached a peak of 3 mV 5 ms after onset and lasted 30 ms [10]. The results with the inhibitory synaptic influence (Fig. 4) show that the output of the neuron was reduced during high frequency stimulation (> 75 Hz).
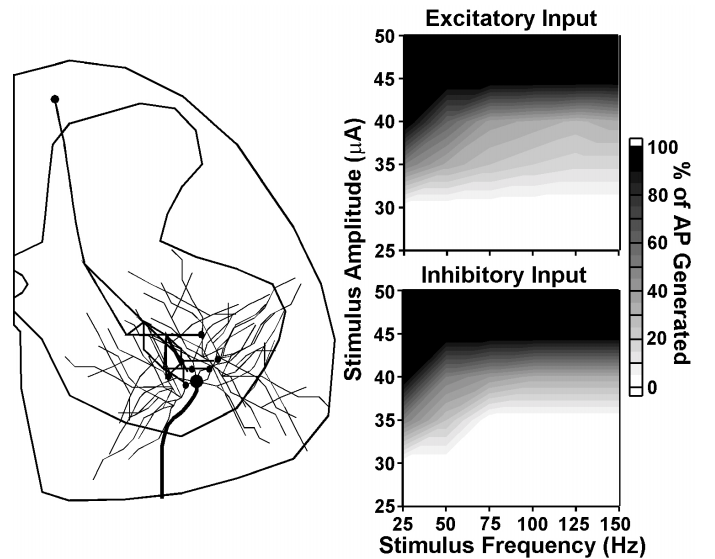
Fig. 4. Influence of synaptic excitation and inhibition on neuronal output. Incorporation of the excitatory input had little effect on the neuronal output map for a symmetrical charge-balanced biphasic stimulus train. Inhibitory input with a time course and magnitude representative of GABAergic inhibition shows that synaptic influences on local cells can affect neuronal output at high frequencies when driven by extracellular sources.

IV. DISCUSSION

Previously we developed asymmetric charge-balanced stimulus waveforms effective in activating targeted neuronal populations, however only single stimuli were considered [5]. In this study we examined the effects of trains of stimuli, which are used in neural prosthetic devices. Studying the effect of stimulus frequency on excitation patterns required models that were able to reproduce accurately the dynamic firing properties of the neurons being stimulated. The neuron models used in this study allowed for the first time, an accurate response to stimulation frequencies greater than 10 Hz, because of the models ability to accurately reproduce the shape and magnitude of the depolarizing and hyperpolarizing afterpotentials. Differences in the afterpotentials of cell body and myelinated axon allowed for enhanced activation of fibers of passage with high stimulus frequencies (Fig. 2). The results demonstrate that manipulation of the non-linear conductances of the neural membrane can enable selective activation of targeted neuronal

populations, and this manipulation can be accomplished by alterations in the stimulus waveform as well as the stimulus frequency.

The results also provide insight into the effect of stimulus frequency on the arrest of tremor by high-frequency stimulation of the thalamus (deep brain stimulation (DBS)). At higher frequencies (> 80 Hz) tremor is suppressed, with a nadir in the stimulus amplitude-frequency tuning curve at ~ 125 Hz [11]. There are large numbers of pre-synaptic GABAergic fibers in the thalamus [12], and activation of these fibers by high frequency stimulus trains may inhibit tremor activity in post-synaptic thalamocortical cells via IPSP summation and decreases in the membrane resistance [13]. This hypothesis is supported by the fact that GABAergic IPSPs have a time course that match well with maximal summation occurring at stimulus frequencies where DBS is most effective (Fig. 4). The GABAergic IPSP reaches it maximum conductance ~5 ms after onset and last for ~30 ms [10]. Therefore, with the ~2 ms delay from excitation of the pre-synaptic fiber to onset of the IPSP in the post-synaptic fiber there exists a peak effectiveness at ~140 Hz for IPSP summation. While the mechanisms regulating the therapeutic effects of DBS are not clear, the results of this study showing that high frequency stimulation enhances the selective activation of fibers of passage and that the summation of GABAergic IPSPs on local cells is maximal at ~140 Hz, suggest that the principal effects of high frequency extracellular thalamic stimulation are synaptically-mediated suppression of local cells and direct excitation of fibers of passage.

V. CONCLUSIONS

The results demonstrate three main conclusions: 1) Differences in the after potentials, and post action potential excitability of the neuronal cell bodies compared to fibers of passage allowed for alterations in stimulus frequency enabled selective activation of fibers of passage. 2) Alterations in the stimulus waveform enabled selective activation of either cells near the electrode or fibers of passage in a realistic neuroprosthetic application. and 3) The selective stimulation waveforms are effective when used in a stimulus train. In addition, preliminary results point toward indirect (synaptic) activation of cells as a possible influence to exploit for selective stimulation.

AKNOWLEDGEMENTS

REFERENCES

[1] J.B. Ranck, "Which elements are excited in electrical stimulation of mammalian central nervous system: A review," *Brain Res.*, vol. 98, pp. 417-440, 1975.

[2] B. Gustafsson, and E. Jankowska, "Direct and indirect activation of nerve cells by electrical pulses applied extracellularly," *J. Physiol.*, vol. 258, pp. 33-61, 1976.

[3] H. Barbeau, D.A. McCrea, M.J. O'Sonovan, S. Rossignol, W.M. Grill, and M.A. Lemay, "Tapping into spinal circuits to restore motor function," *Brain Res. Rev.*, vol. 30, pp. 27-51, 1999.

[4] C.C. McIntyre, and W.M. Grill, "Excitation of central nervous system neurons by nonuniform electric fields," *Biophys. J.*, vol. 76, pp. 878-888, 1999.

[5] C.C. McIntyre, and W.M. Grill, "Selective microstimulation of central nervous system neurons," *Ann. Biomed. Eng.*, vol. 28, pp. 219-233, 2000.

[6] E.N. Warman, W.M. Grill, and D. Durand, "Modeling the effects of electric fields on nerve fibers: determination of excitation thresholds," *IEEE Trans. Biomed. Eng.*, vol. 39, pp. 1244-1254, 1992.

[7] I. Nadelhaft, W.C. Degroat, and C. Morgan, "Location and morphology of parasympathetic preganglionic neurons in the sacral spinal cord of the cat revealed by retrograde axonal transport of horseradish peroxidase," *J. Comp. Neurol.*, vol. 193, pp. 265-281, 1980.

[8] K.B. Thor, C. Morgan, I. Nadelhaft, M. Houston, and W.C. De Groat, "Organization of afferent and efferent pathways in the pudendal nerve of the female cat," *J. Comp. Neurol.*, vol. 288, pp. 263-279, 1989.

[9] R.E. Burke, "Group Ia synaptic input to fast and slow twitch motor units of cat triceps surae," *J. Physiol.*, vol. 196, pp. 605-630, 1968.

[10] R. Miles, and R.K. Wong, "Unitary inhibitory synaptic potentials in the guinea-pig hippocampus in vitro," *J. Physiol.*, vol. 356, pp. 97-113, 1984.

[11] A.L. Benabid, P. Pollak, C. Gervason, D. Hoffmann, D.M. Gao, M. Hommel, J.E. Perret, and J. de Rougemont, "Long-term suppression of tremor by chronic stimulation of the ventral intermediate thalamic nucleus," *Lancet*, vol. 337, pp. 403-406, 1991.

[12] E. Shink, and Y. Smith, "Differential synaptic innervation of neurons in the internal and external segments of the globus pallidus by the GABA- and glutamate-containing terminals in the squirrel monkey," *J. Comp. Neurol.*, vol. 358, pp. 119-141, 1995.

[13] A. Benazzouz, B. Piallat, P. Pollak, and A.L. Benabid, "Responses of substantia nigra pars reticulata and globus pallidus complex to high frequency stimulation of the subthalamic nucleus in rats: electrophysiological data," *Neurosci. Lett.*, vol. 189, pp. 77-80, 1995.